Abrasive machining of ductile iron with CBN

In this paper by **K. Tuffy and M. O' Sullivan**, The performance of a CBN abrasive in an electroplated tool is quantified when high speed grinding ductile iron in terms of specific grinding energy, cutting forces and spindle power requirement. The range of operation of the product was defined in the range of specific material removal rate up to 220 mm³/mm/s, therefore operating under high efficiency deep grinding conditions. An initial ranking is developed by comparing the performance of this CBN with another commercially available abrasive type, with a different impact strength and thermal stability. The mode of tool failure is different and is identified in this paper. The tool life was defined as the amount of material removed before a specific normal force level of 90 N/mm was reached. It was found there was a direct correlation between force and power and either could indicate the end of tool life once a target value was specified. The tool life of the stronger CBN product was twice that of the other weaker abrasive type, which required higher specific grinding energies and grinding forces over the range of material removal rates studied.

In 2002 ductile iron accounted for 31% of casting shipments from 13.14 billion tons in the US. Although pressure pipes are a large portion of this market components for the car, truck and power transmission sectors account for 27% of these ductile iron shipments [1]. Ductile iron or spheroidal graphite iron (SGI) has many properties such as good strength to weight ratio, excellent damping characteristics, good wear resistance and fatigue strength including good machinability [2]. Austempered ductile iron (ADI) is thought to offer all the benefits of ductile iron as well as superior mechanical properties common to many steel forgings and castings with lower manufacturing costs and offers potential for weight savings and associated reduced fuel consumptions costs for example in the automotive industry [3]. ADI is thought to machine similar to high-strength ductile irons [4]. Typical application areas for ductile iron include crankshafts, camshafts, piston liners, gears, piston rings, wheel hubs, manifolds, shafts, railway wheels and other applications such as machine frames and suspension brackets.

An excellent review was given by Inasaki et. al [5] in 1993 which indicated the direction of fixed abrasive processing or grinding preferring the term 'abrasive machining.' The continued growth and development of vitrified bonds has extended the productivity barriers of many high volume automotive and aerospace component producers [6]. Central to the success of the rapidly developing technology is the superabrasive products and product offerings, in particular with regard to CBN [7]. The emphasis on processes such as high efficiency deep grinding (HeDG) has firmly focused the spotlight on the unexplored potential of monolayer CBN wheels and the performance benefits [8]. The HeDG grinding process has been the focus of intensive research from a

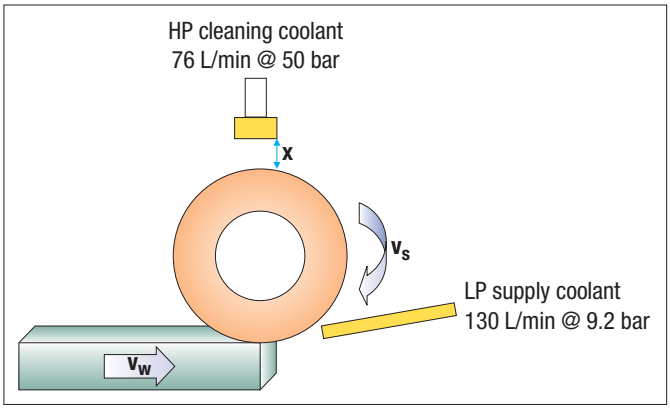

Fig 1a
Schematic of grinding arrangement on Blohm Profimat MT 408

Fig 1b
Close up of surface of electroplated CBN wheel used in this project

Test Conditions - Various CBN B181	
Wheel speed, v_s (m/s)	100
Workpiece speed, v_w (mm/min)	100 to 13,200
Depth of cut, a_e (mm)	1
Coolant - Emulsion (%)	4
Workpiece	EN GJS 700-2 (FCD 700-2 or D7003)
Delivery	LP cooling 9.2bar, HP cleaning 50bar
Wheel type	1A1 - 250(20(127 (b_s = 10)

Table 1 Standard grinding test condition

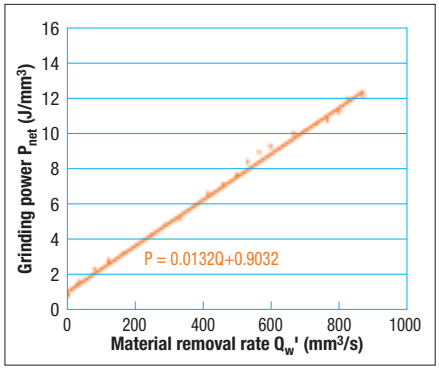

Fig 2 Variation in P_{net} versus Q_w for product A

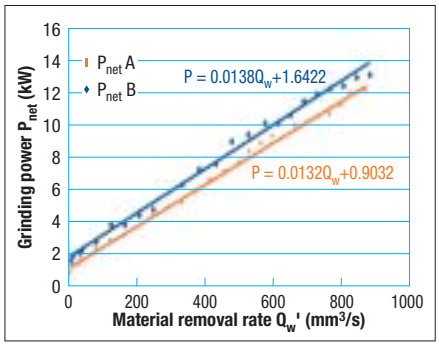

Fig 3 Comparison between product A and product B in terms of P_{net}

process point of view, with an intensive effort on thermal modelling and workpiece subsurface integrity [9]. This paper will concentrate on the abrasive product; with two CBN grade types offered by Element Six reviewed in a high material removal rate application on a pearlitic SGI variant with electroplated CBN. In a follow up paper the grindability of this pearlitic SGI material will be compared with a high strength ADI product.

Test setup

The following tests were carried out on a Blohm Profimat MT 408 with a 45 kW spindle motor with a maximum speed of 8300 rpm. Coolant was supplied as shown in Fig 1 at 9 bar using a Brinkmann impeller pump and Brinkmann screw pump was used to deliver coolant at 50 bar to a cleaning nozzle. The coolant used was a 4% emulsion (Hocut 3380). The distance, x between the cleaning head and the wheel was kept constant. The up-grinding mode is depicted in Fig 1 was chosen for this test. In general for creep feed grinding, down-grinding requires lower specific energies and cutting forces due to the chip formation process but is less efficient in terms of cooling. As Q_w' increases the efficiency of chip formation increases also and the cooling and lubrication aspects of the grinding process become more dominant. Down-grinding is more efficient in terms of cooling, lubrication and swarf removal and was therefore chosen for this investigation.

A step grinding method was employed in this process using half the wheel width, allowing the other half of the wheel to be used as a reference. The standard set of grinding conditions chosen can be seen in Table 1. The purpose of this research was to investigate the process performance with different abrasive types, therefore issues such as platability will be largely ignored. It will be assumed that the only difference between the electroplated tools will be the abrasive type.

The power was recorded directly from the Sinumerik controller and the forces were monitored using a Kistler three component force dynamometer and attendant data acquisition system. In this test the limit for the specific normal force was 90 N/mm and this was called the end of tool life. The surface integrity was checked at this specific normal force level and no obvious phase transformations were evident indicating that the workpiece has not suffered from thermal damage. The dominant pearlitic structure was still evident. Microhardness measurements revealed no thermal softening and/or rehardening had taken place. Given the efficient removal of heat from the workpiece in the form of a stream of sparks it was thought that the workpiece would have tolerated a much higher level of F_n', however this is outside the scope of this investigation.

Discussion – from a superabrasive machining point of view

In order to evaluate any grinding product in a specific process it is reasonable to evaluate the performance range of the product and to attempt to assess what limits the product performance. In superabrasive machining the change in specific grinding energy (u) and the net power consumption (P_{net}) over a wide range of specific material removal rate values (Q_w') are extremely informative. The test conditions used can be viewed in Table 1. Product A is a brownish CBN product, with a predominant tetrahedral morphology and with an impact strength typically 30% greater than product B. Product B is an amber product with a more predominant cubic/octahedral morphology and is not as thermally stable.

Power and specific grinding energy

Fig 2 details the variation in the net power consumption with material removal rate (Q_w) for product A. The P_{net} being defined as the total power less the power consumed in driving the spindle plus the coolant supply when grinding only air. Any reference to power from here will refer to P_{net}. It is clear a relationship exists with:

$$P_{net} = P_o + xQ \qquad (1)$$

Where P_o is the intercept. The slope of the line, x has units of u since the resultant must be equivalent to W (or J/s). The limit of the slope is thought to be the melting energy of the cast iron, which is essentially similar to that of unalloyed iron. The intercept can be taken as a measure of the efficiency of the cutting action of the abrasive since a lower value for this constant will infer a lower P_{net}. Likewise it is believed replacing the emulsion with a neat oil for example will also reduce the value of P_o.

The comparative performance of the two abrasive types A and B is shown in Fig 3 in terms of P_{net}. Here product B has a larger intercept and slightly larger value for the slope of the line over the range of values studied therefore demands a higher level of power, and this

difference increases as Q_w is increased. It is important to note that the wheel condition is assumed to be constant over the full range of Q_w evaluated for both products A and B.

Fig 4 details the variation in the u with Q_w' for product A. The u is seen to decrease with increasing material removal rate. In the present representation no reference is made to the variation in wheel wear with increasing material removal rate. However at increased values of Q_w' a more efficient grinding operation is clearly taking place. Relatively less ploughing and sliding are taking place at higher Q_w' and in the limit where the u approaches the minimum specific energy for chip formation, the ploughing and sliding energies would then be zero. The specific grinding energy is insensitive to alloying and heat treatment since the melting energy of the material is independent of this [10] – it is very important to consider this for high material removal rate applications and helps explain when HeDG can operate for materials with a relatively low grindability.

A power law expression of the form $u = AQ_w'^{-b}$ is expressed where A is a constant and b is the exponent describing the curve. The constant A is thought to be dependent on the workpiece material and its resistance to shear whereas the exponent is thought to be more related to the chip formation process [11]. It is worth stating that such curve exponents can only compare two different products under the same process conditions if the range of values being considered are the same. Fig 5 shows the difference in the grinding efficiency between the two abrasives – product A and B. Such a curve is less informative if the Q_w' is increased by both the a_e and v_w in a surface grinding operation since these curves will be largely independent.

Increasing Q_w' resulted in a more efficient grinding process. Interestingly at low Q_w' the product B required a much higher u in comparison to product A. Abrasive A with its dominant tetrahedral morphology has a distinctive angular shape with a relatively larger aspect ratio. Bailey and Juchem [7] state that CBN products with a more tetrahedral morphology require lower grinding powers and produce lower cutting forces. It is clear that product A with its sharper cutting action has a power law relationship with a lower constant value and exponent. It is thought the sharpness of the abrasive is critical in determining the magnitude of this constant and exponent, as well as the ability of the abrasive to maintain this sharpness. It is appreciated that most characterisation is done at the macro-level with respect to the abrasive and not at the micro level where the active cutting point or plane is transient. In addition the shape of the abrasive does not necessarily mean it will be presented to the workpiece in this manner – this will be determined by the lay of the particle in the tool making process. At higher Q_w' values the relative larger chip height may mean the size effect is less dominant but at low Q_w' the size effect becomes dominant and therefore the sharpness of the abrasive becomes critical. Of course at higher Q_w' the number of active particles changes also.

Variation in the grinding forces with increasing Q_w'

Fig 6 details the change in the specific normal (F_n') and the specific tangential forces (F_t') over the corresponding range of Q_w'. At low Q_w' there is little difference in the specific normal and tangential components of the force measured, however at higher Q_w' the stronger, more tetrahedral product A has a distinctly lower specific normal and tangential component in comparison to product B.

In fact for a given force level for product B, say, F_n' = 80 N/mm, almost a 10% greater Q_w' is achievable producing the same F_n' with product A.

Variation in the surface finish over a range of Q_w'

The change in surface finish of the ductile iron workpiece with increasing Q_w' in terms of R_a and R_z can be seen in Fig 7. What is surprising initially is that the magnitude of the R_a and R_z is as great at low Q_w' as it is at high Q_w', particularly in the case of product A. The chip height equation tends to predict that at increasing chip height (as Q_w' increases) an increase in the roughness parameters would be expected. However the surface topography of the grinding wheel is changing continuously and despite this occurring only on the micro level it will have a significant bearing on the resultant grinding action and hence the surface finish of the workpiece. This partly explains why high surface finish values were obtained at low Q_w' since these were ground first using a relatively newer and hence coarser grinding wheel.

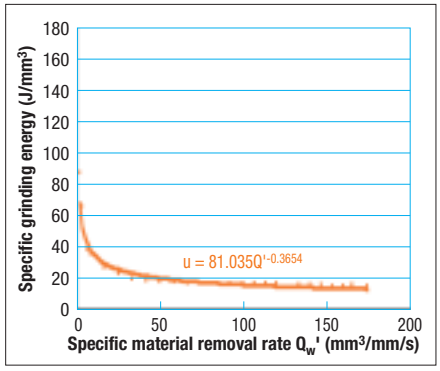

Fig 4 Variation in the u with Q_w' for product A

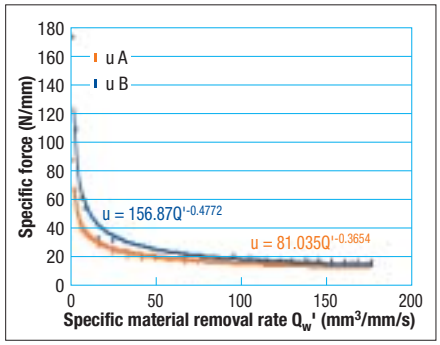

Fig 5 Comparison between product A and product B in terms of u

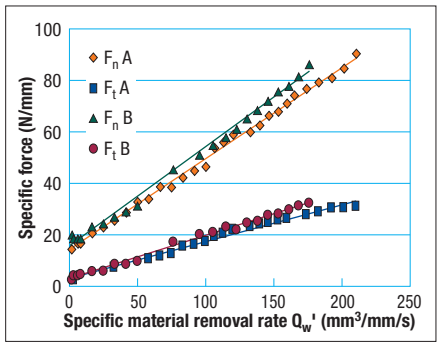

Fig 6 Specific force comparison between product A and product B

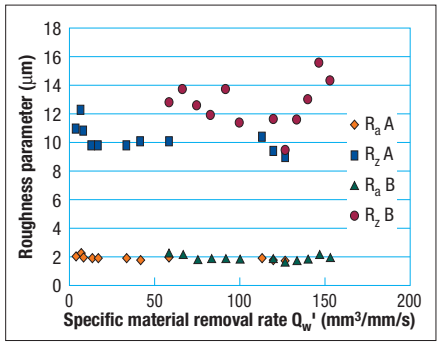

Fig 7 Variation in surface finish with increasing Q_w' for product A and B

Also a relatively inefficient grinding operation is taking place at low Q_w' and the size distribution (B181) of the abrasive product would indicate that it is more suited to a roughing type operation. The surface finish produced by product A is superior to product B. This will be further discussed later in this article.

Continuous monitoring at a Q_w' = 100 mm³/mm/s

The change in specific forces produced when machining ductile iron with product A at a Q_w' of 100 mm³/mm/s with cumulative volume removed is shown in Fig 8. A freshly plated wheel was used for this test. It is clear over the initial 500 cm³ a transient behaviour is observed. This is characteristic of an electroplated tool showing a 'settling in' period where the topography of the grinding wheel is altering to achieve a more collective uniform grit height of protrusion. This will be further referred to later in this article. It is worth noting that the specific normal force value in the steady state is almost double the value it started out when the new wheel was used. An almost constant force level is then reached and this is preserved for a sustained period of time emphasising the high strength of the product. For the purposes of this test program a specific force level of 90 N/mm was specified as the end of tool life. This value can therefore be thought as arbitrary and or as an accelerated tool life test.

The difference in the performance between product A and B in terms of the transient behaviour and duration of the relatively steady state period can be seen in Fig 9. Both products have a similar specific normal and tangential force value at the start of the test indicating that this value is indeed dictated by the kinematic roughness on the grinding wheel and not the particles themselves. The performance of product B is almost devoid of any steady state period with an approximate linear increase in the specific forces after a specific volume (V_w') of 100,000 mm³/mm of GGG 70 is machined. This is in complete contrast to the product A, with on average a 30% stronger impact strength as measured by the Friatest. The tool life of product A is almost double that of product B according to the specification of the tool life. From analysis of the surface topography of the grinding wheels the resultant wear levels were still under 13 microns, meaning that the tools would have continued to grind for a much longer time, if the tool life was dictated by the wear on the particles or the radial wheel wear.

A more appropriate way in terms of a production environment of monitoring tool life in electroplated tools is by monitoring the spindle power since this can be more easily achieved without the need for installation of secondary transducers. Fig 10 shows that the P_{net} can be directly related to the forces in grinding and is an excellent indicator of the end of tool life. The machine output or gross spindle power is simply a constant plus P_{net} so interpreting the machine output is also very straightforward once the value of the power is determined where the end of tool life is reached. Depending on the given operation or application, this may be the power level at which the surface integrity of the workpiece becomes unacceptable or simply the power level at which the tool becomes unusable due to the excessive wear on the grinding wheel.

Variation in workpiece surface finish with cumulative volume of workpeice machined

The products are specified by a particle size distribution but also have a shape distribution. The combination of these two factors means following the electroplating process there will be a spread of particle heights of protrusion of the CBN particles on the wheel hub. Of course the shape of the particle will also affect the lay of particle on the wheel hub but many manufacturers can now control this. A large spread of particle height of protrusion will result in a sharply acting grinding wheel, consuming low grinding power and producing a relatively rough surface topography on the workpiece. Fig 11 details the variation in the surface topography with reference only to R_a and R_z with increasing V_w'. Again a constant Q_w' of 100 mm³/mm/s with product A was used for this assessment. After an initial grinding period the R_a and the R_z decrease substantially. This suggests a finer grinding wheel surface with a more controlled height of protrusion. The production of a finer surface finish on the workpiece correlates with an increase in the specific grinding forces (and of course the spindle power). It can therefore be concluded that the grinding wheel surface does actually change quite significantly over the duration of the test.

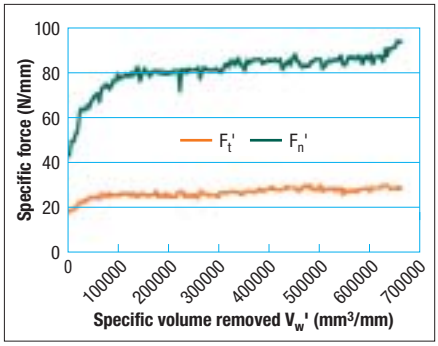

Fig 8 Variation in the specific forces for product A with increasing volume removed

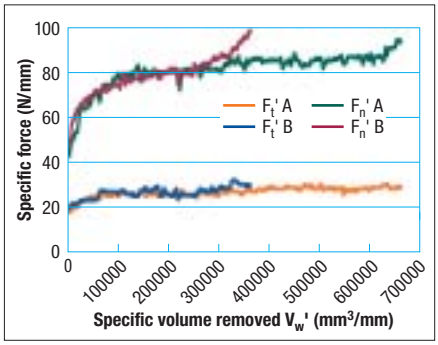

Fig 9 Specific force progression for product A and product B

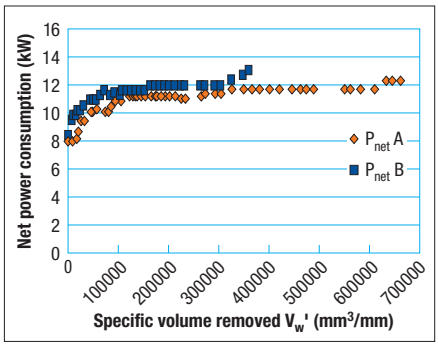

Fig 10 Change in net spindle power with cumulative volume of workpiece removed

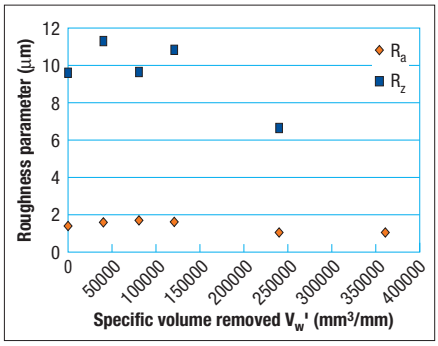

Fig 11 Change in surface roughness with cumulative volume ground for product A

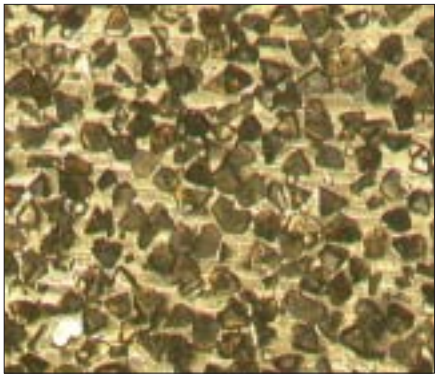

Fig 12 Image of grinding wheel produced with product A prior to final test

Fig 13 Electroplated CBN wheels for this project were supplied by Cranden Diamond Products

It is worth stating that no wheel loading was observed at any point. The image in Fig 12 shows a section of the grinding wheel surface produced with product A 50,000 mm^3/mm prior to the end of the tool life test. No wheel loading is visible that would have contributed to an increase in power consumption. With a few exceptions the abrasive particles are relatively unworn, with no wear flats and little abrasive loss from the bond matrix.

Conclusion

Selecting the correct product for a specified process and application is critical to achieving the most economic processing route. It is clearly evident that product A in this analysis contributed to significantly increasing tool life. It can be expected that the reduced grinding forces would produce components with a superior surface integrity. The superior performance of product A is due to a greater impact resistance as well as a tetrahedral morphology. It is recognised that this research was completed independent of the production complexities in the electroplating process. The spindle power is an excellent process control tool, capable of indicating the end of tool life with excellent correlation with the grinding forces in an electroplated application. The surface finish of the workpiece changes significantly during the lifetime of an electroplated grinding wheel, but in particular during the early transient or settling in period. The duration of this period will depend on the process conditions, workpiece grindability and the abrasive type. ◆

Nomenclature

Q_w	Material removal rate (mm^3/s)
Q_w'	Specific material removal rate ($mm^3/mm/s$)
u	Specific grinding energy (J/mm^3)
P	Nett power in grinding (kW)
F_t'	Specific tangential grinding force (N/mm)
F_n'	Specific normal grinding force (N/mm)
V_w'	Specific volume of workpiece removed (mm^3/mm)
v_s	Wheel speed (m/s)
v_w	Workpiece speed (mm/min)
a_e	Depth of cut (mm)
b_s	Width of grinding wheel (mm)
R_a	Average surface roughness (μm)
R_z	Mean roughness depth (μm)

Acknowledgements

The authors of this paper would like to thank Cranden Diamond Products Ltd. for the production of electroplated CBN wheels used in this project (Fig 13). In addition the private communication with Dipl. -Ing H.O. Juchem and Professor Brian Rowe and was much appreciated.

This article is based on a paper presented at the 1st International Industrial Diamond Conference held in Barcelona, Spain in October 2005 and is printed with kind permission of Diamond At Work Ltd.

References

[1] Kirgin K.H., (2003), Castings in the Global Market, AFS Metalcasting Forecast and Trends 2002.

[2] Cast Irons, (1996), Ohio: ASM International.

[3] Warrick R.J., Althoff P., Druschitz A.P., Lemke J., Zimmerman K. Mani P.H. and Rackers M.L., (2000), Austempered Ductile Iron Castings for Chassis Applications, Proceedings SAE 2000-01-1290.

[4] www.kennametal.com

[5] Inasaki I., Tönshoff H.K. and Howes T.D., (1993), Abrasive Machining in the Future, Annals of CIRP, Vol 42-2, pp. 723-732.

[6] Wolter H., A New Generation of Highly Porous Vitrified Bond CBN Grinding Wheels, Industrial Diamond Review, Issue 3 1996, pp 68-70.

[7] Bailey M. and Juchem H.O., The advantages of CBN grinding: low cutting forces and improved workpiece integrity, Industrial Diamond Review, Issue 3 1998, pp. 83-89.

[8] Stephenson D.J., Corbett J., Laine E., Johnstone I. and Baldwin A., (2001), Burn Threshold Studies for Superabrasive Grinding using Electroplated CBN Wheels, Proceedings of the Society of Manufacturing Engineers, MR01-219.

[9] Jin T. and Stephenson D.J., (2004), Three Dimensional Finite Element Simulation of Transient Heat Transfer in High Efficiency Deep Grinding, Annals of CIRP, Vol. 53-1, pp. 259-262.

[10] Malkin S., (1989), Grinding Technology, Theory and Applications of Machining with Abrasives, Wiley, New York.

[11] Marinescu I.D., Rowe W. B., Dimitrov B and Inasaki I., (2004), Tribology of Abrasive Machining Processes, William Andrew Publishing.

Appendix

In this paper, Product A refers to Element Six standard product ABN 800 and Product B to ABN 300.

Authors

K. Tuffy and M. O'Sullivan work for Element Six Ltd, Shannon Airport, Co Clare, Ireland. www.e6.com